NeuroImage 235 (2021) 118002

Contents lists available at ScienceDirect

NeuroImage

journal homepage: www.elsevier.com/locate/neuroimage

Anatomical bases of fast parietal grasp control in humans: A diffusion-MRI tractography study

Nathalie Richard[a,b,1], Michel Desmurget[a,b,1], Achille Teillac[a,b,c], Pierre-Aurélien Beuriat[a,b,d], Lara Bardi[a,b], Gino Coudé[a,b], Alexandru Szathmari[a,b,d], Carmine Mottolese[a,b,d], Angela Sirigu[a,b,2], Bassem Hiba[a,b,2,*]

[a] Institute of Cognitive Neuroscience Marc Jeannerod, CNRS / UMR 5229, 69500 Bron, France
[b] Université Claude Bernard, Lyon 1, 69100 Villeurbanne, France
[c] Institut de neurosciences cognitives et intégratives d'Aquitaine, CNRS / UMR 5287, 33076 Bordeaux, France
[d] Department of Pediatric Neurosurgery, Hôpital Femme Mère Enfant, 69500, Bron, France

ARTICLE INFO

Keywords:
Tractography
Parietal cortex
Grasping
motor control
Feedback
Volition
Humans

ABSTRACT

The dorso-posterior parietal cortex (DPPC) is a major node of the grasp/manipulation control network. It is assumed to act as an optimal forward estimator that continuously integrates efferent outflows and afferent inflows to modulate the ongoing motor command. In agreement with this view, a recent per-operative study, in humans, identified functional sites within DPPC that: (i) instantly disrupt hand movements when electrically stimulated; (ii) receive short-latency somatosensory afferences from intrinsic hand muscles. Based on these results, it was speculated that DPPC is part of a rapid grasp control loop that receives direct inputs from the hand-territory of the primary somatosensory cortex (S1) and sends direct projections to the hand-territory of the primary motor cortex (M1). However, evidence supporting this hypothesis is weak and partial. To date, projections from DPPC to M1 grasp zone have been identified in monkeys and have been postulated to exist in humans based on clinical and transcranial magnetic studies. This work uses diffusion-MRI tractography in two samples of right- ($n = 50$) and left-handed ($n = 25$) subjects randomly selected from the Human Connectome Project. It aims to determine whether direct connections exist between DPPC and the hand control sectors of the primary sensorimotor regions. The parietal region of interest, related to hand control (hereafter designated $DPPC_{hand}$), was defined permissively as the 95% confidence area of the parietal sites that were found to disrupt hand movements in the previously evoked per-operative study. In both hemispheres, irrespective of handedness, we found dense ipsilateral connections between a restricted part of $DPPC_{hand}$ and focal sectors within the pre and postcentral gyrus. These sectors, corresponding to the hand territories of M1 and S1, targeted the same parietal zone (spatial overlap > 92%). As a sensitivity control, we searched for potential connections between the angular gyrus (AG) and the pre and postcentral regions. No robust pathways were found. Streamline densities identified using AG as the starting seed represented less than 5 % of the streamline densities identified from $DPPC_{hand}$. Together, these results support the existence of a direct sensory-parietal-motor loop suited for fast manual control and more generally, for any task requiring rapid integration of distal sensorimotor signals.

1. Introduction

The primate hand is an extraordinarily sophisticated and flexible sensorimotor system. It is able to grasp and manipulate various objects and tools with astonishing precision. For a large part, this skillfulness relies on the contribution of powerful control loops that continuously adjust the ongoing efferent command to compensate for biological (Guigon et al., 2008; Harris and Wolpert, 1998), dynamic (Augurelle et al., 2003; Edin et al., 1992) and contextual (Desmurget and Prablanc, 1997; Paulignan et al., 1991) errors. Typically, these loops are modeled in the form of a real-time optimal controller that steadily drives neural activity in output motor regions, so as to progressively nullify the distance between the ongoing state of the motor plant, indirectly estimated by integrating sensory inflows and motor outflows (Desmurget and Grafton, 2000; Wolpert et al., 1995) and the goal of the movement (Diedrichsen et al., 2010; Todorov, 2004).

* Corresponding author at: Institute of Cognitive Neuroscience Marc Jeannerod, CNRS / UMR 5229, 69500 Bron, France
E-mail address: bassem.hiba@isc.cnrs.fr (B. Hiba).
[1] Both authors contributed equally.
[2] Co-senior authors for this work.

https://doi.org/10.1016/j.neuroimage.2021.118002.
Received 30 September 2020; Received in revised form 26 January 2021; Accepted 24 March 2021
Available online 28 March 2021.

To date, there is still no consensus on the neural circuits involved in the control of these skilled hand actions. In monkey, the grasp/manipulation network is thought to be mediated by a dorsolateral circuit cascading from the hand proprioceptive sector of the parietal operculum (SII region), to the anterior intraparietal area (aIP) to the ventral premotor region (F5) and, finally the primary motor hand region (F1) (Borra et al., 2017; Grafton, 2010; Jeannerod et al., 1995). Converging observations suggest that a similar network exists in humans (Davare et al., 2011; Filimon, 2010; Turella and Lingnau, 2014). During the last decade Transcranial Magnetic Stimulation (TMS) studies have shown, for instance, that transient virtual lesions of the rostral part of the intraparietal sulcus impairs grasping behaviors (Dafotakis et al., 2008; Davare et al., 2007), prevents on-line adjustments of hand shaping (Rice et al., 2007; Rice et al., 2006; Tunik et al., 2005) and bias neural activity in the ventral premotor region (Davare et al., 2010).

However, recent evidence also suggests the existence of a more direct control loop linking the primary sensory cortex (S1) to the dorso-posterior-parietal cortex (DPPC) to the primary motor cortex (M1). In monkeys, anatomical studies have identified direct projections from DPPC to M1 areas controlling hand/arm movements (Borra and Luppino, 2017; Kaas and Stepniewska, 2016; Rizzolatti et al., 1998). A recent study, in particular, reported connections between the grasp regions of DPPC (medial bank of the IPS and area 5) and M1 (Gharbawie et al., 2011). In humans, it was reported that a conditioning-TMS pulse delivered over DPPC could significantly depress motor evoked potentials triggered, in intrinsic hand muscles, by a test pulse delivered over the ipsilateral M1 (Koch et al., 2007; Mackenzie et al., 2016). Likewise, a recent per-operative study recorded short-latency inhibitory effects of superior parietal stimulation on corticospinal excitability of distal upper limb muscles (Cattaneo et al., 2020). Moreover, it has been shown that focal lesions within the superior parietal lobule (SPL) can cause unwanted hand movements through a release of inhibition within M1 (Assal et al., 2007). Regarding sensory inputs, several studies have reported that upper-limb somatosensory evoked potentials recorded in DPPC are abolished following S1 excision (Allison et al., 1991a; Allison et al., 1991b). Consistent with all these observations, we recently identified neural sites, in DPPC, that display the expected properties of a neural on-line sensorimotor controller (Desmurget et al., 2018). First, these sites instantly disrupt ongoing open/close hand movements when electrically stimulated. Second, they receive short-latency somatosensory inputs from intrinsic hand muscles.

To sum up, the results above point to the possible existence of a rapid feedback loop involved in grasp/manipulation control, mediated by neural activity in DPPC, receiving sensory signals from the hand area of S1 and projecting to the hand area of M1 (Fig. 1). This hypothesis was evaluated using diffusion Magnetic Resonance Imaging (dMRI) tractography in two successive samples of right- and left-handed subjects randomly selected from the Human Connectome Project (HCP) database. The dorso-posterior parietal hand control region ($DPPC_{hand}$) was used as the seed region of interest (ROI) for the tractography. This region was defined as the 95% confidence area of the parietal sites that disrupted hand movements in our previous per-operative study (Desmurget et al., 2018) (Fig. 1). To avoid ambiguity, it may be worth mentioning that this area is likely to be oversized, i.e. to be substantially larger than the parietal region truly involved in hand control. Indeed, $DPPC_{hand}$ was computed from a limited number of per-operative points (n = 12) collected in brain tumor patients (Desmurget et al., 2018) known to exhibit a high level of cortical reorganizations (Desmurget et al., 2007). As a consequence, we expect the posterior parietal area connected with M1 and S1 hand regions, if any, to be substantially smaller than our seed parietal region.

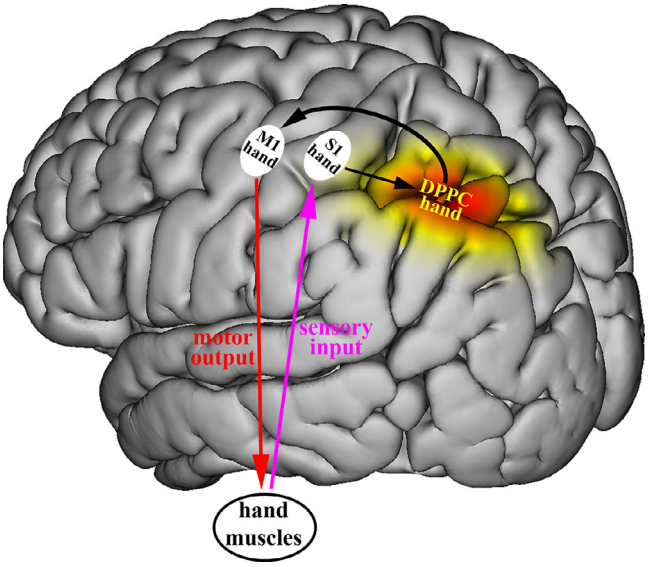

Fig. 1. Putative anatomy of the parietal inhibitory network. S1: primary somatosensory cortex. M1: primary motor cortex. DPPC: dorso-posterior parietal region. Confidence ellipsoid of $DPPC_{hand}$ was computed from the parietal sites where electrical stimulation was found to trigger a selective disruption of hand movements in a previous per-operative study (Desmurget et al., 2018). The yellow border displays the 95% confidence border of this ellipsoid.

2. Material and methods

The HCP is a unique dataset aiming to be used by the scientific community to shed light on the anatomical and functional connectivity of the human brain (Glasser et al., 2013; Van Essen et al., 2013). Tractography analyses were carried out on dMRI multi-shell data of 50 right-handed subjects (22 to 35 years old; 31 females) randomly selected from the HCP database. To evaluate the generality of the results obtained from this main sample and to evaluate the existence of potential hemispheric asymmetries related to handedness, we also considered an additional population of 25 left-handed subjects (randomly selected from the HCP database; 25 to 33 years old; 16 females). The 75 multi-shell data-sets (18 images with b=0 $s.mm^{-2}$ and 270 diffusion-weighted images with b=1000, 2000 and 3000 $s.mm^{-2}$ applied in 90 non-collinear diffusion directions) were acquired with an isotropic spatial resolution of 1.25 mm and corrected for distortion artifacts. (Sotiropoulos et al., 2013). Tissue segmentations as well as cortical pial and white matter surfaces computed for each subject using FreeSurfer (Fischl, 2012) were taken from the structural HCP database.

Within this dataset, precentral (PreC) and postcentral (PostC) ROIs were defined from Destrieux parcellation (Destrieux et al., 2010). The $DPPC_{hand}$ ROI was defined on each individual pial surface, in MNI coordinates, as the 95% confidence area of all the parietal sites that disrupted hand movements when electrically stimulated in our per-operative study (Desmurget et al., 2018). Tractography analyses were performed from the parietal portion of the ellipse (i.e. after the small anterior fraction of the ellipse involving the postcentral gyrus was truncated) (Figs. 1 and S1).

For dMRI tractography, we used the state-of-the-art MRtrix3 software (Tournier et al., 2019). First, for all tissue types (white matter (WM), grey matter (GM) and cerebrospinal fluid) we computed the response function estimations using an automated unsupervised algorithm (Dhollander et al., 2016). Second, we computed the multi-shell, multi-tissue constrained spherical deconvolution (Jeurissen et al., 2014). A whole-brain probabilistic tractogram (Tournier et al., 2010) was then computed with the Anatomically-Constrained Tractography (Smith et al., 2012) and GM / WM interface seeding. We used the ensemble tractography approach (Takemura et al., 2016) with variations of the step size [0.3, 0.6 and 1.25 mm], of the angle [30°, 45° and 60°] and of the cutoff [0.05, 0.1, 0.15] to achieve a 54 million of streamlines tractogram. The final whole brain tractogram of each subject was

automatically filtered to identify the left and right ipsilateral tracts connecting $DPPC_{hand}$ and PostC; and $DPPC_{hand}$ and PreC. This filtering was performed using purely anatomical criteria. Streamlines passing through both ipsilateral $DPPC_{hand}$ and PostC ROIs form the $DPPC_{hand}$/PostC bundle, while the $DPPC_{hand}$/PreC bundle is defined by all streamlines crossing both ipsilateral $DPPC_{hand}$ and the PreC ROIs. Supplementary Table 1 summarizes the average number of streamlines obtained for each of the $DPPC_{hand}$/PostC and $DPPC_{hand}$/PreC bundles.

The end-point density surfaces of $DPPC_{hand}$/PostC and $DPPC_{hand}$/PreC bundles were computed for each subject as the amount of streamlines endpoints projected onto each vortex of white matter surface. Then, the obtained endpoints density surfaces were averaged for all subjects, normalized over the range of 0 to 1 and displayed on the mean pial surface after a heat kernel smoothing (Chung et al., 2005) with a Full Width at Half Maximum (FWHM) of 4.9. The overlap between tracts from pre and postcentral regions within the $DPPC_{hand}$ pial surface was computed using the Jaccard index (intersection over union of both surfaces of interest).

3D-streamlines density maps of $DPPC_{hand}$/PostC and $DPPC_{hand}$/PreC tracts (representing the amount of streamlines traversing each voxel of the brain) were also computed for each subject using track-density imaging (Calamante et al., 2011). Then, the 3D-streamline density maps of $DPPC_{hand}$/PostC tracks and $DPPC_{hand}$/PreC tracts were averaged for all the subjects, normalized over the range of 0 to 1 and overlaid on the T1 study template using the buildtemplateparallel procedure of the ANTS toolkit (Avants et al., 2011). These tracks were then compared with the three subdivisions of the superior longitudinal fasciculi (SLF) bundles included in the white matter atlas of the FSL XTRACT toolbox (https://fsl.fmrib.ox.ac.uk/fsl/fslwiki/XTRACT) (Warrington et al., 2020), thresholded at 10 % of the maximal probability.

As a methodological sensitivity control of the tractography approach used in this study, we replicated all the analyses above to investigate the Angular Gyrus AG/PostC and AG/PreC connectivity. The AG ROI used for tractography was defined as the inferior part of the angular gyrus from Destrieux's parcellation (Destrieux et al., 2010) situated outside the $DPPC_{hand}$ (supplementary Figure S1). AG was selected in light of converging evidence suggesting that this area has only sparse direct connections with the primary sensorimotor areas (Koch et al., 2010; Schulz et al., 2015; Seghier, 2013).

All ROIs ($DPPC_{hand}$, AG, PostC and PreC) are available on request to the corresponding author.

3. Results

3.1. Main analyses: right-handed subjects

As illustrated in Fig. 2, which displays the mean normalized density maps of streamline endpoints projected to the average pial surface, streamlines from $DPPC_{hand}$ converge within circumscribed areas of the pre- and postcentral gyri (see supplementary Table 2 for MNI coordinates of the centers of gravity of these projections; see also supplementary Fig. S2 for more views of these endpoint surface densities). These areas are in the sector of the sensorimotor strip where hand/finger movements are typically represented (Desmurget et al., 2014; Guzzetta et al., 2007; Kuhtz-Buschbeck et al., 2008; Penfield and Boldrey, 1937; Szameitat et al., 2012). More precisely, they are close the middle knee of the central lobe (Ribas, 2010), an anatomical marker that is typically assumed to define the functional hot-spot for distal hand control, both in the primary motor (Vigano et al., 2019; Yousry et al., 1997) and the primary sensorimotor (Sastre-Janer et al., 1998; White et al., 1997) cortex. These pre and postcentral regions of maximum density are located, respectively, within M1 (Brodmann area 4) and S1 (mainly Brodmann area 2, with some extension into area 1; see Fig. 2 and supplementary Fig. S2). Supplementary Fig. S3 further illustrates these results by showing streamline bundles ($DPPC_{hand}$/PreC, $DPPC_{hand}$/PostC) and density of streamline endpoints for three randomly selected subjects.

Consistent with the predictions of our initial hypothesis (Fig. 1) and the results of our previous per-operative study (Desmurget et al., 2018), streamlines identified in PreC and PostC originated in the same subregion of our initial parietal seed ROI (Fig. 3 and supplementary Fig. S4). Within this subregion (hereafter designated $sDPPC_{hand}$), spatial overlap between pre and postcentral streamlines was extensive. It reached 92.2% and 92.4% for the left and right hemispheres respectively. Also, in both hemispheres, the center of gravity of $sDPPC_{hand}$ was located in the anterior part of the intraparietal sulcus (aIP; supplementary Table 2). As a control, we compared the sum of streamlines density for PostC/PreC and $sDPPC_{hand}$. We found no statistical difference, in agreement with the conclusion that the fibre projections found in $sDPPC_{hand}$ reflect the sum of the projections identified in PostC and PreC (sign test; Left hemisphere $p > .65$, Right hemisphere $p > .10$).

Overall, these results are also consistent with the claim that our seed parietal area was oversized (see introduction). Indeed, $sDPPC_{hand}$ appears substantially smaller than $DPPC_{hand}$ (Left: 55% of the seed surface; Right: 64%). Its centre of gravity is also slightly shifted in the dorso-anterior direction, along IPS (Left: 17 mm; Right: 16 mm).

Finally, it may be worth noting that no sign of lateralization was visible in our data. The total number of streamlines was statistically comparable in the left and right hemispheres for both bundles ($sDPPC_{hand}$/PostC and $sDPPC_{hand}$/PreC, sign test, ps > .10; see supplementary Table 3 for details).

When the analyses above were replicated with AG as the seed ROI instead of $DPPC_{hand}$, very few streamlines were identified (as expected from previous studies; see methods). Streamline densities measured from AG to PostC and from AG to PreC represented less than 5% of the streamline densities identified from $DPPC_{hand}$. This difference was unlikely to be related to differences in the size of the two ROIs. Indeed, as shown by additional analyses, AG and $DPPC_{hand}$ have comparable surfaces (47 cm^2 and 49 cm^2 respectively).

3.2. Supplementary analyses: left-handed subjects

Analyses involving the second sample of left-handed subjects fully replicated the conclusions above. As shown in Fig. 4, we found dense ipsilateral connections between a restricted area in the anterior part of $DPPC_{hand}$ and focal sectors within PreC (M1; Brodmann area 4) and PostC (S1; Brodmann area 2 with some extension into area 1) hand territories (see supplementary Table 4 for MNI coordinates of the centers of gravity of these projections; see also supplementary Figure S5). This parietal subregion ($sDPPC_{hand}$) was substantially smaller than our initial seed region (Left: 60% of the seed surface; Right: 62%). Within $sDPPC_{hand}$, we found a strong overlap between streamlines originating from pre and post central structures (Left hemisphere: 92.5%; Right hemisphere: 95.2%; Fig. 5 and supplementary Figure S6). In addition, there was no statistical difference between the sum of streamlines density found in PostC/PreC and $sDPPC_{hand}$ (sign test; Left hemisphere $p > .10$, Right hemisphere $p > .40$).

In agreement with the results obtained in right-handed subjects, tractography revealed no significant sign of lateralization in this sample of left-handed individuals. The total number of streamlines was statistically comparable in the left and right hemispheres for both bundles (sign test, ps > .20; see supplementary Table 3 for details). We conducted additional analyses to identify potential asymmetries between right- and left-handed subjects. Again, no significant difference was found. The total number of streamlines of the two bundles ($sDPPC_{hand}$/PostC and $sDPPC_{hand}$/PreC) was statistically comparable in each hemisphere between the two samples (Kolmogorov-Smirnov two-sample test, ps > .10; see supplementary Table 5 for details).

4. Discussion

To summarize, our results identify an anatomical network linking the cortical territories devoted to hand control in the primary motor,

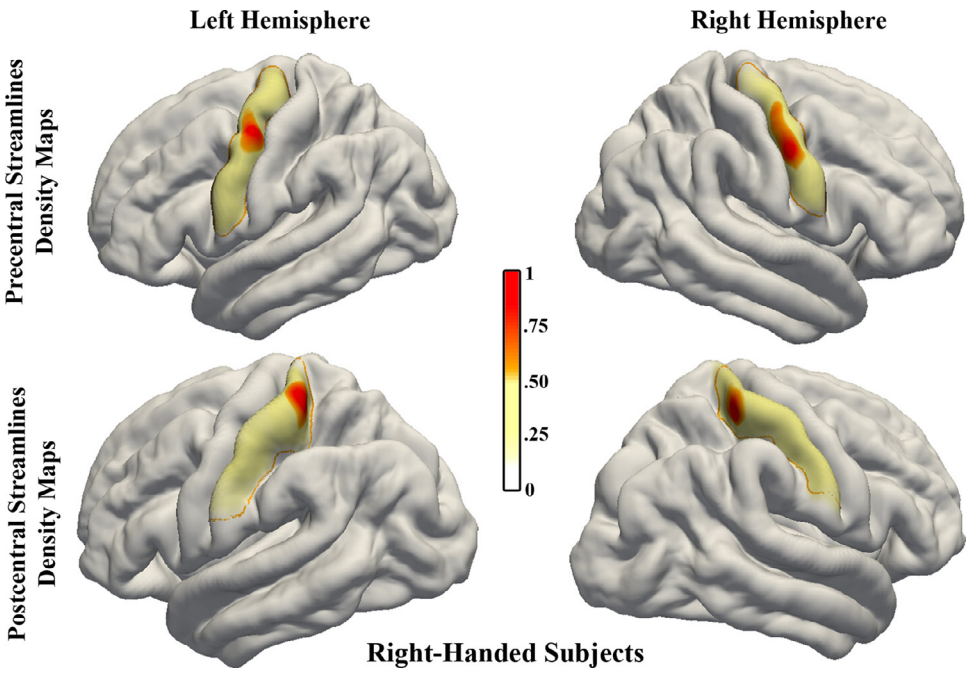

Fig. 2. Right-handed subjects. Mean normalized density maps of streamline endpoints projected from $DPPC_{hand}$ to PreC and PostC ROIs of the average pial surface. The orange lines represent the 90 % borders of the streamline density map. Note that the four panels of the figure were oriented to maximize the visibility of the results. Complementary views with different orientations are shown in supplementary Figure S2.

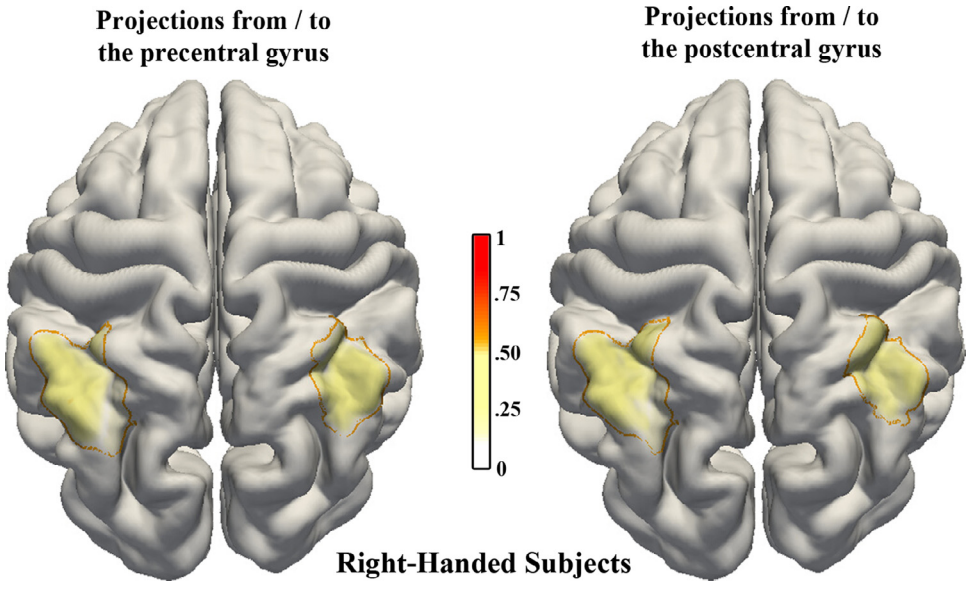

Fig. 3. Right-handed subjects. Mean normalized density maps of streamline endpoints projected from PreC and PostC to the $DPPC_{hand}$ ROI of the average pial surface. The orange lines represent the 90 % borders of the streamline density map. Note that the two panels of the figure were oriented to maximize the visibility of the results. Complementary views with different orientations are shown in supplementary figures S4.

the primary somatosensory and the dorso-posterior parietal areas. This network provides the required architecture for the existence of a functional, short-latency, sensory-parietal-motor loop dedicated to the rapid control of hand movements.

Of interest with respect to this conclusion is the degree to which grasping/manipulation behaviors differ from reaching activities. In humans, aIP is clearly linked to fine distal control. Convergent evidence have shown that permanent (anatomical) and transient (TMS-induced) lesions within this region disrupt the grasp component of prehension movements, without affecting the transport phase (Binkofski et al., 1998; Rice et al., 2007; Rice et al., 2006; Tunik et al., 2005). The ongoing control of this transport phase has been shown to rely on the medial intraparietal sulcus (mIP) (Chib et al., 2009; Desmurget et al., 1999) and/or the SPL (Desmurget et al., 2001; Diedrichsen et al., 2005; Wolpert et al., 1998). Several modeling experiments have also established the computational viability of dissociating the neural representations of distal (grasp-manipulation) and proximal (limb transport) movement components for object-oriented actions (Hoff and Arbib, 1993; Ulloa and Bullock, 2003).

However, in contrast with this dissociative view, many neuroimaging studies have reported reach related activity in the human aIP, irrespective of any grasping behavior (for a review, Filimon, 2010). In addition, it was found that the so-called hand-knob was not as selective as initially described by Penfield (Penfield and Boldrey, 1937; Penfield and Rasmussen, 1950). Within this area, distal (wrist/finger) and proximal (arm/forearm) representations overlap generously (Branco et al., 2003; Desmurget et al., 2014; Desmurget and Sirigu, 2015). Moreover, in the present study, although parietal streamlines were concentrated around the hand-knob in M1 and S1, diffuse projections were identified medially and laterally with respect to this knob (yellow gradients in Figures 2, 4, S2 and S5). Based on these observations, it cannot be determined whether the functional network identified in the present study is selectively associated with fine distal motor control or whether it is involved

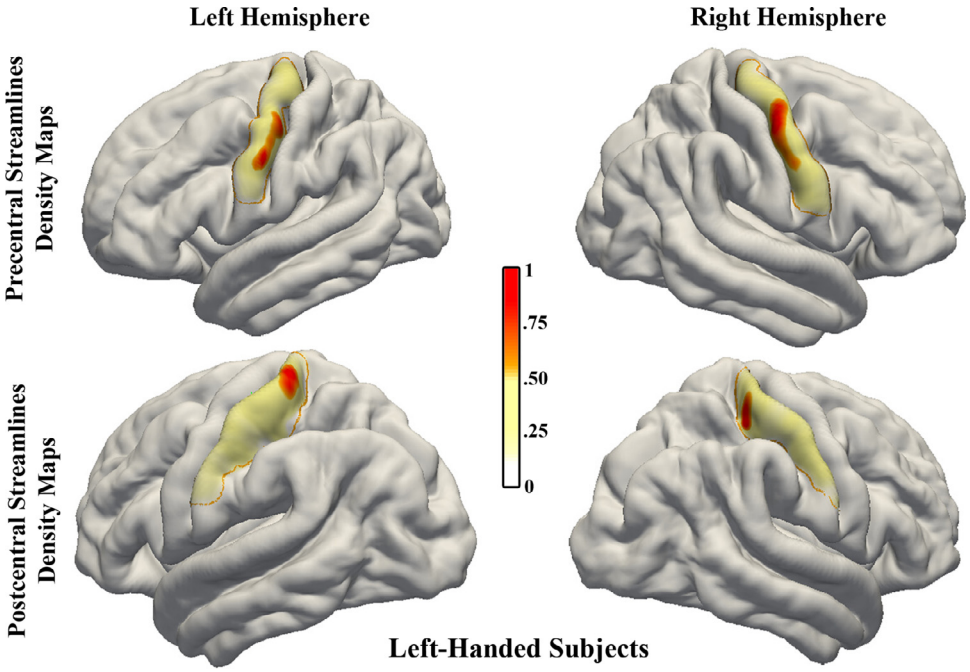

Fig. 4. Left-handed subjects. Same data and conventions as Fig. 2. Complementary views with different orientations are shown in supplementary figures S5.

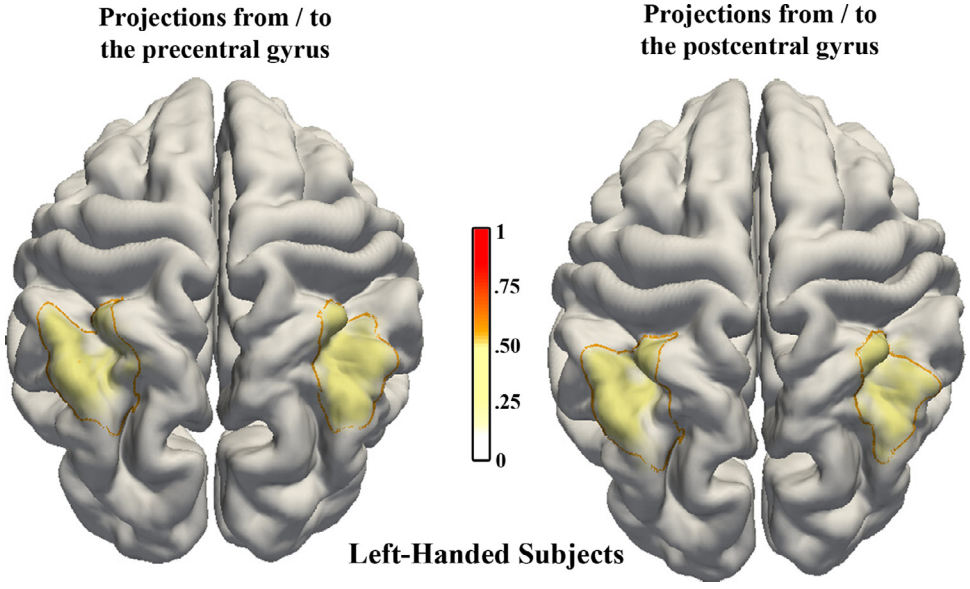

Fig. 5. Left-handed subjects. Same data and conventions as Fig. 3. Complementary views with different orientations are shown in supplementary Fig. S6.

in the regulation of more general proximo-distal reach-to-grasp activities.

In connection with this issue, it may be worth mentioning that the parietal region here defined as $sDPPC_{hand}$ is a complex structure (Andersen et al., 2014; Freedman and Ibos, 2018; Janssen and Scherberger, 2015). Certainly, as emphasized in the introduction, it plays a central role in motor planning and control (for a recent review, Sirigu and Desmurget, 2020). However, it is also a key node of many other functional networks involved in action selection (Lindner, 2018), spatial attention (Corbetta and Shulman, 2002), coordinate transformations (Andersen et al., 1997), multisensory integration (Huang et al., 2012), crossmodal evaluations (Grefkes et al., 2002), etc. As a consequence, the role of the direct anatomical connections here identified between $sDPPC_{hand}$ and S1 and $sDPPC_{hand}$ and M1 is unlikely to be restricted to on-line motor control. For instance, this pathway could be involved in haptic object processing. Indeed, convergent data suggest that $sDPPC_{hand}$ contribute to this function through combining somatosensory and motor information (Burton et al., 2008; James et al., 2007; Sathian, 2016).

Another key point to be discussed concerns the novelty of our results. The sensory-parietal and motor-parietal tracts identified in this study are part of the superior longitudinal system (SLS) recently described by Mandonnet and colleagues (Mandonnet et al., 2018). This system comprises the three branches of the SLF (SLF-I to III) (Catani and Thiebaut de Schotten, 2012; Parlatini et al., 2017; Schmahmann and Pandya, 2006). Based on this observation, we performed specific analyses to determine more precisely whether the pathways isolated in the present study are part of a specific branch of the SLF. To this end, for the right-hand sample, we superimposed our $sDPPC_{hand}$/PostC and $sDPPC_{hand}$/PreC bundles with the three subdivisions of the SLF tract, using the white matter atlas available through the XTRACT toolbox (Warrington et al., 2020; see methods). As illustrated in Fig. 6, the longitudinal portion of the

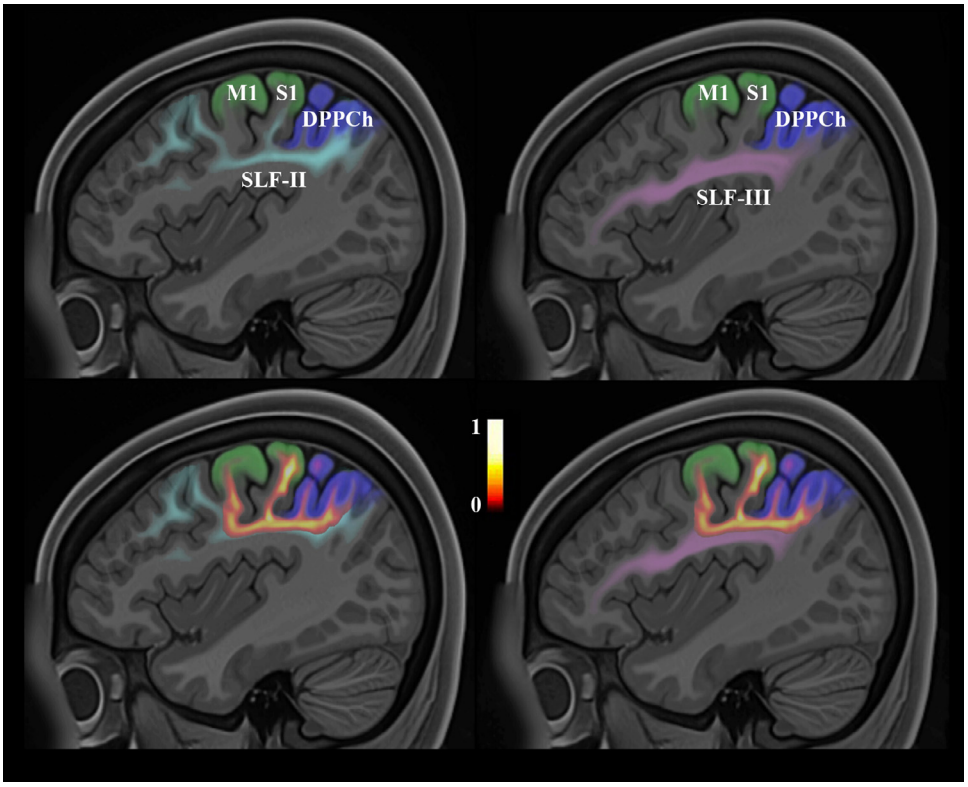

Fig. 6. Top row: Middle (SLF-II; left panel, light blue tract) and Ventral (SLF III; right panel, purple tract) branches of the superior longitudinal fasciculus (SLF) from the XTRACT toolbox (Warrington et al., 2020) overlaid on a sagittal view of the mean T1 template computed from all the subjects. Bottom row: Mean normalized streamline density maps of $DPPC_{hand}$ ($DPPC_h$; dark blue) to PreC (M1 area, green) and PostC (S1 area, green) tracts superimposed on SLF II (left panel) and SLF III (right panel) branches. Most of the overlap occurs with SLF-II (75%). Figure computed from the right-handed sample. See text for details.

$sDPPC_{hand}$/PostC and $sDPPC_{hand}$/PreC bundles closely follow the SLF tract. 75% of the overlap occurs with SLF-II. This is much more than the percentages found for SLF-III (22 %) and SLF-I (3%). Anatomically, SLF-II originates from the posterior-inferior parietal region and predominantly targets the dorsal premotor cortex and dorsolateral prefrontal cortex (Catani and Thiebaut de Schotten, 2012; Parlatini et al., 2017; Schmahmann and Pandya, 2006). This tract has been associated with various functions, including motor control, spatial attention and some aspects of language production (Hecht et al., 2015; Parlatini et al., 2017; Thiebaut de Schotten et al., 2014; Wang et al., 2016). Our data extend these observations by suggesting that the connections here identified between specific cortical territories devoted to hand control in M1, S1 and DPPC, run through the SLF-II bundle. Of course, further studies are now required to confirm this hypothesis.

In the present study, based on tractograms, we failed to identify asymmetries: (i) between the right and left hemispheres for a given hand preference (right or left); and (ii) between right- and left-handed participants for a given hemisphere (right or left). This result is consistent with TMS experiments showing a strict contralateral control for grasping movements (Rice et al., 2007). It is also supported, at group level, by previous studies showing no relation between handedness and hemispheric asymmetry, for SLF-II (Budisavljevic et al., 2017; Hecht et al., 2015; Howells et al., 2018; Makris et al., 2005). However, contradictory observations have been reported (Wang et al., 2016) and one cannot exclude that our sample size was not large enough to allow identification of discrete interhemispheric asymmetries. As a consequence, this negative result should be considered with caution until further studies are conducted.

Finally, an important methodological issue needs to be raised. It is known that tractography algorithms tend to produce a substantial amount of false-positive bundles (Maier-Hein et al., 2017). However, the hypothesis-driven model used in this research dramatically minimizes this risk of erroneous identification. As shown in several studies, while tractography might produce disputable conclusions when used in isolation (David et al., 2019), it represents a powerful cross-validation tool when used predictively, in conjunction with other techniques such as functional MRI (Guye et al., 2003), histology (Dell'Acqua et al., 2013), polarized light imaging (Mollink et al., 2017), tract-tracing (Jbabdi et al., 2013), deep brain stimulation (Calabrese, 2016) or direct electrical stimulation (Kamada et al., 2009). In relation to this point, one may mention our inability to identify robust pathways using AG as the seed ROI. Together with previous studies showing sparse direct connections between AG and primary sensorimotor areas (Koch et al., 2010; Schulz et al., 2015; Seghier, 2013), this result pleads against the conclusion that the sensory-parietal-motor tracks identified in this study reflect false positive reconstructions of the tractography procedure. Whether the few streamlines identified in this study between AG and primary sensorimotor regions reflect false positive or real sparse connections (Koch et al., 2010; Schulz et al., 2015; Seghier, 2013) cannot be determined from this study.

To summarize, this study identifies a direct anatomical loop connecting the cortical territories harboring hand representations in the primary motor, primary somatosensory and dorso-posterior parietal cortices. This loop is suited for fast manual control and more generally, any task requiring rapid integration of distal sensorimotor signals. Whether the circuit we identified should be considered a new branch of the SLF-II needs to be confirmed.

CediT authorship contribution statement

Nathalie Richard: Conceptualization, Methodology, Software, Writing-original draft. Michel Desmurget: Conceptualization, Methodology, Writing-original draft. Achille Teillac: Methodology, Software, Visualization. Pierre-Aurélien Beuriat: Conceptualization, Validation, Review & Editing. Lara Bardi: Validation, Software, Review & Editing. Gino Coudé: Methodology, Review & Editing. Alexandru Szathmari: Validation, Review & Editing. Carmine Mottolese: Validation, Review & Editing. Angela Sirigu: Conceptualization, Writing-original draft, Supervision, Funding acquisition. Bassem Hiba: Conceptualization, Writing-original draft, Supervision, Funding acquisition.

Declaration of Competing Interest

The authors declare no conflict of interest.

Funding

This work was supported by the Centre National de la Recherche Scientifique (CNRS), the Agence Nationale de la Recherche (ANR-16-CE37-0017-01) and the Laboratory of Excellence programs CORTEX (ANR-11-LABX-0042 Université de Lyon) and TRAIL (ANR-10-LABX-57 Université de Bordeaux).

Data availability

All MRI data used in this study are available in the HCP open access dataset. All the software used are open source code. The data that support the findings of this study are available from the corresponding author, BH, upon reasonable request.

Supplementary materials

Supplementary material associated with this article can be found, in the online version, at doi:10.1016/j.neuroimage.2020.117520.

References

Allison, T., McCarthy, G., Wood, C.C., Jones, S.J., 1991a. Potentials evoked in human and monkey cerebral cortex by stimulation of the median nerve. A review of scalp and intracranial recordings. Brain 114 (Pt 6), 2465–2503.
Allison, T., Wood, C.C., McCarthy, G., Spencer, D.D., 1991b. Cortical somatosensory evoked potentials. II. Effects of excision of somatosensory or motor cortex in humans and monkeys. J. Neurophysiol. 66, 64–82.
Andersen, R.A., Andersen, K.N., Hwang, E.J., Hauschild, M., 2014. Optic ataxia: from Balint's syndrome to the parietal reach region. Neuron 81, 967–983.
Andersen, R.A., Snyder, L.H., Bradley, D.C., Xing, J., 1997. Multimodal representation of space in the posterior parietal cortex and its use in planning movements. Annu. Rev. Neurosci. 20, 303–330.
Assal, F., Schwartz, S., Vuilleumier, P., 2007. Moving with or without will: functional neural correlates of alien hand syndrome. Ann. Neurol. 62, 301–306.
Augurelle, A.S., Smith, A.M., Lejeune, T., Thonnard, J.L., 2003. Importance of cutaneous feedback in maintaining a secure grip during manipulation of hand-held objects. J. Neurophysiol. 89, 665–671.
Avants, B.B., Tustison, N.J., Song, G., Cook, P.A., Klein, A., Gee, J.C., 2011. A reproducible evaluation of ANTs similarity metric performance in brain image registration. Neuroimage 54, 2033–2044.
Binkofski, F., Dohle, C., Posse, S., Stephan, K.M., Hefter, H., Seitz, R.J., et al., 1998. Human anterior intraparietal area subserves prehension: a combined lesion and functional MRI activation study. Neurology 50, 1253–1259.
Borra, E., Gerbella, M., Rozzi, S., Luppino, G., 2017. The macaque lateral grasping network: A neural substrate for generating purposeful hand actions. Neurosci. Biobehav. Rev. 75, 65–90.
Borra, E., Luppino, G., 2017. Functional anatomy of the macaque temporo-parieto-frontal connectivity. Cortex 97, 306–326.
Branco, D.M., Coelho, T.M., Branco, B.M., Schmidt, L., Calcagnotto, M.E., Portuguez, M., et al., 2003. Functional variability of the human cortical motor map: electrical stimulation findings in perirolandic epilepsy surgery. J. Clin. Neurophysiol. 20, 17–25.
Budisavljevic, S., Dell'Acqua, F., Zanatto, D., Begliomini, C., Miotto, D., Motta, R., et al., 2017. Asymmetry and structure of the fronto-parietal networks underlie visuomotor processing in humans. Cereb. Cortex 27, 1532–1544.
Burton, H., Sinclair, R.J., McLaren, D.G., 2008. Cortical network for vibrotactile attention: a fMRI study. Hum. Brain Mapp. 29, 207–221.
Calabrese, E., 2016. Diffusion tractography in deep brain stimulation surgery: a review. Front. Neuroanat. 10.
Calamante, F., Tournier, J.-D., Heidemann, R.M., Anwander, A., Jackson, G.D., Connelly, A., 2011. Track density imaging (TDI): Validation of super resolution property. Neuroimage 56, 1259–1266.
Catani, M., Thiebaut de Schotten, M., 2012. Atlas of Human Brain Connections. Oxford University Press, New York.
Cattaneo, L., Giampiccolo, D., Meneghelli, P., Tramontano, V., Sala, F., 2020. Cortico–cortical connectivity between the superior and inferior parietal lobules and the motor cortex assessed by intraoperative dual cortical stimulation. Brain Stimul. 13, 819–831.
Chib, V.S., Krutky, M.A., Lynch, K.M., Mussa-Ivaldi, F.A., 2009. The separate neural control of hand movements and contact forces. J. Neurosci. 29, 3939–3947.
Chung, M.K., Robbins, S.M., Dalton, K.M., Davidson, R.J., Alexander, A.L., Evans, A.C., 2005. Cortical thickness analysis in autism with heat kernel smoothing. Neuroimage 25, 1256–1265.
Corbetta, M., Shulman, G.L., 2002. Control of goal-directed and stimulus-driven attention in the brain. Nat. Rev. Neurosci. 3, 201–215.
Dafotakis, M., Sparing, R., Eickhoff, S.B., Fink, G.R., Nowak, D.A., 2008. On the role of the ventral premotor cortex and anterior intraparietal area for predictive and reactive scaling of grip force. Brain Res. 1228, 73–80.
Davare, M., Andres, M., Clerget, E., Thonnard, J.L., Olivier, E., 2007. Temporal dissociation between hand shaping and grip force scaling in the anterior intraparietal area. J. Neurosci. 27, 3974–3980.
Davare, M., Kraskov, A., Rothwell, J.C., Lemon, R.N., 2011. Interactions between areas of the cortical grasping network. Curr. Opin. Neurobiol. 21, 565–570.
Davare, M., Rothwell, J.C., Lemon, R.N., 2010. Causal connectivity between the human anterior intraparietal area and premotor cortex during grasp. Curr. Biol 20, 176–181.
David, S., Heemskerk, A.M., Corrivetti, F., Thiebaut de Schotten, M., Sarubbo, S., Corsini, F., et al., 2019. The superoanterior fasciculus (SAF): a novel white matter pathway in the human brain? Front. Neuroanat. 13, 24.
Dell'Acqua, F., Bodi, I., Slater, D., Catani, M., Modo, M., 2013. MR diffusion histology and micro-tractography reveal mesoscale features of the human cerebellum. Cerebellum 12, 923–931.
Desmurget, M., Bonnetblanc, F., Duffau, H., 2007. Contrasting acute and slow-growing lesions: a new door to brain plasticity. Brain 130, 898–914.
Desmurget, M., Epstein, C.M., Turner, R.S., Prablanc, C., Alexander, G.E., Grafton, S.T., 1999. Role of the posterior parietal cortex in updating reaching movements to a visual target. Nat. Neurosci. 2, 563–567.
Desmurget, M., Grafton, S.T., 2000. Forward modeling allows feedback control for fast reaching movements. Trends Cogn. Sci. 4, 423–431.
Desmurget, M., Grea, H., Grethe, J.S., Prablanc, C., Alexander, G.E., Grafton, S.T., 2001. Functional anatomy of nonvisual feedback loops during reaching: a positron emission tomography study. J. Neurosci. 21, 2919–2928.
Desmurget, M., Prablanc, C., 1997. Postural control of three-dimensional prehension movements. J. Neurophysiol. 77, 452–464.
Desmurget, M., Richard, N., Beuriat, P.A., Szathmari, A., Mottolese, C., Duhamel, J.R., et al., 2018. Selective inhibition of volitional hand movements after stimulation of the dorsoposterior parietal cortex in humans. Curr. Biol. 28, 3303–3309 e3303.
Desmurget, M., Richard, N., Harquel, S., Baraduc, P., Szathmari, A., Mottolese, C., et al., 2014. Neural representations of ethologically relevant hand/mouth synergies in the human precentral gyrus. Proc. Natl. Acad. Sci. USA 111, 5718–5722.
Desmurget, M., Sirigu, A., 2015. Revealing humans' sensorimotor functions with electrical cortical stimulation. Philos. Trans. R. Soc. Lond. B Biol. Sci. 370, 20140207.
Destrieux, C., Fischl, B., Dale, A., Halgren, E., 2010. Automatic parcellation of human cortical gyri and sulci using standard anatomical nomenclature. Neuroimage 53, 1–15.
Dhollander, T., Raffelt, D., Connelly, A., 2016. Unsupervised 3-tissue response function estimation from single-shell or multi-shell diffusion MR data without a co-registered T1 image. ISMRM Workshop on Breaking the Barriers of Diffusion MRI.
Diedrichsen, J., Hashambhoy, Y., Rane, T., Shadmehr, R., 2005. Neural correlates of reach errors. J. Neurosci. 25, 9919–9931.
Diedrichsen, J., Shadmehr, R., Ivry, R.B., 2010. The coordination of movement: optimal feedback control and beyond. Trends Cogn. Sci. 14, 31–39.
Edin, B.B., Westling, G., Johansson, R.S., 1992. Independent control of human finger-tip forces at individual digits during precision lifting. J. Physiol. 450, 547–564.
Filimon, F., 2010. Human cortical control of hand movements: parietofrontal networks for reaching, grasping, and pointing. Neuroscientist 16, 388–407.
Fischl, B., 2012. FreeSurfer. Neuroimage 62, 774–781.
Freedman, D.J., Ibos, G., 2018. An integrative framework for sensory, motor, and cognitive functions of the posterior parietal cortex. Neuron 97, 1219–1234.
Gharbawie, O.A., Stepniewska, I., Qi, H., Kaas, J.H., 2011. Multiple parietal-frontal pathways mediate grasping in macaque monkeys. J. Neurosci. 31, 11660–11677.
Glasser, M.F., Sotiropoulos, S.N., Wilson, J.A., Coalson, T.S., Fischl, B., Andersson, J.L., et al., 2013. The minimal preprocessing pipelines for the human connectome project. Neuroimage 80, 105–124.
Grafton, S.T., 2010. The cognitive neuroscience of prehension: recent developments. Exp. Brain Res. 204, 475–491.
Grefkes, C., Weiss, P.H., Zilles, K., Fink, G.R., 2002. Crossmodal processing of object features in human anterior intraparietal cortex: an fMRI study implies equivalencies between humans and monkeys. Neuron 35, 173–184.
Guigon, E., Baraduc, P., Desmurget, M., 2008. Computational motor control: feedback and accuracy. Eur. J. Neurosci. 27, 1003–1016.
Guye, M., Parker, G.J., Symms, M., Boulby, P., Wheeler-Kingshott, C.A., Salek-Haddadi, A., et al., 2003. Combined functional MRI and tractography to demonstrate the connectivity of the human primary motor cortex in vivo. Neuroimage 19, 1349–1360.
Guzzetta, A., Staudt, M., Petacchi, E., Ehlers, J., Erb, M., Wilke, M., et al., 2007. Brain representation of active and passive hand movements in children. Pediatr. Res. 61, 485–490.
Harris, C.M., Wolpert, D.M., 1998. Signal-dependent noise determines motor planning. Nature 394, 780–784.
Hecht, E.E., Gutman, D.A., Bradley, B.A., Preuss, T.M., Stout, D., 2015. Virtual dissection and comparative connectivity of the superior longitudinal fasciculus in chimpanzees and humans. Neuroimage 108, 124–137.
Hoff, B., Arbib, M.A., 1993. Models of trajectory formation and temporal interaction of reach and grasp. J. Mot. Behav. 25, 175–192.
Howells, H., Thiebaut de Schotten, M., Dell'Acqua, F., Beyh, A., Zappala, G., Leslie, A., et al., 2018. Frontoparietal tracts linked to lateralized hand preference and manual specialization. Cereb. Cortex 28, 2482–2494.
Huang, R.S., Chen, C.F., Tran, A.T., Holstein, K.L., Sereno, M.I., 2012. Mapping multisensory parietal face and body areas in humans. Proc. Natl. Acad. Sci. USA 109, 18114–18119.
James, T.W., Kim, S., Fisher, J.S., 2007. The neural basis of haptic object processing. Can. J. Exp. Psychol. 61, 219–229.

Janssen, P., Scherberger, H., 2015. Visual guidance in control of grasping. Annu. Rev. Neurosci. 38, 69–86.
Jbabdi, S., Lehman, J.F., Haber, S.N., Behrens, T.E., 2013. Human and monkey ventral prefrontal fibers use the same organizational principles to reach their targets: tracing versus tractography. J. Neurosci. 33, 3190–3201.
Jeannerod, M., Arbib, M.A., Rizzolatti, G., Sakata, H., 1995. Grasping objects: the cortical mechanisms of visuo-motor transformations. Trends Neurosci. 18, 314–320.
Jeurissen, B., Tournier, J.D., Dhollander, T., Connelly, A., Sijbers, J., 2014. Multi-tissue constrained spherical deconvolution for improved analysis of multi-shell diffusion MRI data. Neuroimage 103, 411–426.
Kaas, J.H., Stepniewska, I., 2016. Evolution of posterior parietal cortex and parietal-frontal networks for specific actions in primates. J. Comp. Neurol. 524, 595–608.
Kamada, K., Todo, T., Ota, T., Ino, K., Masutani, Y., Aoki, S., et al., 2009. The motor-evoked potential threshold evaluated by tractography and electrical stimulation. J. Neurosurg. 111, 785–795.
Koch, G., Cercignani, M., Pecchioli, C., Versace, V., Oliveri, M., Caltagirone, C., et al., 2010. In vivo definition of parieto-motor connections involved in planning of grasping movements. Neuroimage 51, 300–312.
Koch, G., Fernandez Del Olmo, M., Cheeran, B., Ruge, D., Schippling, S., Caltagirone, C., et al., 2007. Focal stimulation of the posterior parietal cortex increases the excitability of the ipsilateral motor cortex. J. Neurosci. 27, 6815–6822.
Kuhtz-Buschbeck, J.P., Gilster, R., Wolff, S., Ulmer, S., Siebner, H., Jansen, O., 2008. Brain activity is similar during precision and power gripping with light force: an fMRI study. Neuroimage 40, 1469–1481.
Lindner, A., 2018. Motor control: parietal stimulation prevents voluntary hand movement. Curr. Biol. 28, R1200–R1202.
Mackenzie, T.N., Bailey, A.Z., Mi, P.Y., Tsang, P., Jones, C.B., Nelson, A.J., 2016. Human area 5 modulates corticospinal output during movement preparation. Neuroreport 27, 1056–1060.
Maier-Hein, K.H., Neher, P.F., Houde, J.C., Cote, M.A., Garyfallidis, E., Zhong, J., et al., 2017. The challenge of mapping the human connectome based on diffusion tractography. Nat. Commun. 8, 1349.
Makris, N., Kennedy, D.N., McInerney, S., Sorensen, A.G., Wang, R., Caviness Jr., V.S., et al., 2005. Segmentation of subcomponents within the superior longitudinal fascicle in humans: a quantitative, in vivo, DT-MRI study. Cereb. Cortex 15, 854–869.
Mandonnet, E., Sarubbo, S., Petit, L., 2018. The nomenclature of human white matter association pathways: proposal for a systematic taxonomic anatomical classification. Front. Neuroanat. 12, 94.
Mollink, J., Kleinnijenhuis, M., Cappellen van Walsum, A.-M.v., Sotiropoulos, S.N., Cottaar, M., Mirfin, C., et al., 2017. Evaluating fibre orientation dispersion in white matter: comparison of diffusion MRI, histology and polarized light imaging. Neuroimage 157, 561–574.
Parlatini, V., Radua, J., Dell'Acqua, F., Leslie, A., Simmons, A., Murphy, D.G., et al., 2017. Functional segregation and integration within fronto-parietal networks. Neuroimage 146, 367–375.
Paulignan, Y., Jeannerod, M., MacKenzie, C., Marteniuk, R., 1991. Selective perturbation of visual input during prehension movements. 2. The effects of changing object size. Exp. Brain Res. 87, 407–420.
Penfield, W., Boldrey, E., 1937. Somatic motor and sensory representation in the cerebral cortex of man as studied by electrical stimulation. Brain 60, 389–443.
Penfield, W., Rasmussen, T., 1950. The Cerebral Cortex of Man. MacMillan, New York.
Ribas, G.C., 2010. The cerebral sulci and gyri. Neurosurg. Focus 28, E2.
Rice, N.J., Tunik, E., Cross, E.S., Grafton, S.T., 2007. On-line grasp control is mediated by the contralateral hemisphere. Brain Res. 1175, 76–84.
Rice, N.J., Tunik, E., Grafton, S.T., 2006. The anterior intraparietal sulcus mediates grasp execution, independent of requirement to update: new insights from transcranial magnetic stimulation. J. Neurosci. 26, 8176–8182.
Rizzolatti, G., Luppino, G., Matelli, M., 1998. The organization of the cortical motor system: new concepts. Electroencephalogr. Clin. Neurophysiol. 106, 283–296.
Sastre-Janer, F.A., Regis, J., Belin, P., Mangin, J.F., Dormont, D., Masure, M.C., et al., 1998. Three-dimensional reconstruction of the human central sulcus reveals a morphological correlate of the hand area. Cereb. Cortex 8, 641–647.
Sathian, K., 2016. Analysis of haptic information in the cerebral cortex. J. Neurophysiol. 116, 1795–1806.
Schmahmann, J.D., Pandya, D.N., 2006. Fiber Pathways of the Brain. Oxford university Press, New York.
Schulz, R., Koch, P., Zimerman, M., Wessel, M., Bonstrup, M., Thomalla, G., et al., 2015. Parietofrontal motor pathways and their association with motor function after stroke. Brain 138, 1949–1960.
Seghier, M.L., 2013. The angular gyrus: multiple functions and multiple subdivisions. Neuroscientist 19, 43–61.
Sirigu, A., Desmurget, M., 2020. The Functional Organization of Posterior Parietal Cortex in Humans. In: Kaas, J., Krubitzer, L. (Eds.), The Senses, 2nd Edition. Elsevier, Amsterdam.
Smith, R.E., Tournier, J.D., Calamante, F., Connelly, A., 2012. Anatomically-constrained tractography: improved diffusion MRI streamlines tractography through effective use of anatomical information. Neuroimage 62, 1924–1938.
Sotiropoulos, S.N., Jbabdi, S., Xu, J., Andersson, J.L., Moeller, S., Auerbach, E.J., et al., 2013. Advances in diffusion MRI acquisition and processing in the Human Connectome Project. Neuroimage 80, 125–143.
Szameitat, A.J., Shen, S., Conforto, A., Sterr, A., 2012. Cortical activation during executed, imagined, observed, and passive wrist movements in healthy volunteers and stroke patients. Neuroimage 62, 266–280.
Takemura, H., Caiafa, C.F., Wandell, B.A., Pestilli, F., 2016. Ensemble Tractography. PLoS Comput. Biol. 12, e1004692.
Thiebaut de Schotten, M., Tomaiuolo, F., Aiello, M., Merola, S., Silvetti, M., Lecce, F., et al., 2014. Damage to white matter pathways in subacute and chronic spatial neglect: a group study and 2 single-case studies with complete virtual "in vivo" tractography dissection. Cereb. Cortex 24, 691–706.
Todorov, E., 2004. Optimality principles in sensorimotor control. Nat. Neurosci. 7, 907–915.
Tournier, J.D., Calamante, F., Connelly, A., 2010. Improved probabilistic streamlines tractography by 2nd order integration over fibre orientation distributions. Proc. Int. Soc. Magn. Reson. Med..
Tournier, J.D., Smith, R., Raffelt, D., Tabbara, R., Dhollander, T., Pietsch, M., et al., 2019. MRtrix3: a fast, flexible and open software framework for medical image processing and visualisation. Neuroimage 202, 116137.
Tunik, E., Frey, S.H., Grafton, S.T., 2005. Virtual lesions of the anterior intraparietal area disrupt goal-dependent on-line adjustments of grasp. Nat. Neurosci. 8, 505–511.
Turella, L., Lingnau, A., 2014. Neural correlates of grasping. Front. Hum. Neurosci. 8, 686.
Ulloa, A., Bullock, D., 2003. A neural network simulating human reach-grasp coordination by continuous updating of vector positioning commands. Neural Netw. 16, 1141–1160.
Van Essen, D., Smith, S., Barch, D., Behrens, T., Yacoub, E., Ugurbil, K., 2013. The WU-Minn human connectome project: an overview. Neuroimage 80, 62–79.
Vigano, L., Fornia, L., Rossi, M., Howells, H., Leonetti, A., Puglisi, G., et al., 2019. Anatomo-functional characterisation of the human "hand-knob": a direct electrophysiological study. Cortex 113, 239–254.
Wang, X., Pathak, S., Stefaneanu, L., Yeh, F.C., Li, S., Fernandez-Miranda, J.C., 2016. Subcomponents and connectivity of the superior longitudinal fasciculus in the human brain. Brain Struct. Funct. 221, 2075–2092.
Warrington, S., Bryant, K.L., Khrapitchev, A.A., Sallet, J., Charquero-Ballester, M., Douaud, G., et al., 2020. XTRACT - Standardised protocols for automated tractography in the human and macaque brain. Neuroimage 217, 116923.
White, L.E., Andrews, T.J., Hulette, C., Richards, A., Groelle, M., Paydarfar, J., et al., 1997. Structure of the human sensorimotor system. I: morphology and cytoarchitecture of the central sulcus. Cereb. Cortex 7, 18–30.
Wolpert, D.M., Ghahramani, Z., Jordan, M.I., 1995. An internal model for sensorimotor integration. Science 269, 1880–1882.
Wolpert, D.M., Goodbody, S.J., Husain, M., 1998. Maintaining internal representations: the role of the human superior parietal lobe. Nat. Neurosci. 1, 529–533.
Yousry, T.A., Schmid, U.D., Alkadhi, H., Schmidt, D., Peraud, A., Buettner, A., et al., 1997. Localization of the motor hand area to a knob on the precentral gyrus. A new landmark. Brain 120 (Pt 1), 141–157.